Resistor-Based Temperature Sensors: A Technical Review

Yong Tae Lee[1], Woo Jun Choi[2], Young Cheol Chae[a]
Department of Electrical and Electronic Engineering, Yonsei University
E-mail: [1]2016314133@yonsei.ac.kr, [2]dnwns777@yonsei.ac.kr

***Abstract* – This paper presents a technical overview of recently developed resistor-based temperature sensors, which achieve high energy-efficiency and high resolution, simultaneously. Such sensors consist of silicided polysilicon resistors that have relatively high temperature coefficients (TCs), low 1/*f* noise, low supply dependency, and low stress sensitivity. Various design techniques of resistor-based sensors are compared and their performances are summarized.**

***Keywords*— CMOS temperature sensor, Energy-efficiency, High resolution, Resistor-based temperature sensor, Silicided polysilicon resistors.**

I. INTRODUCTION

The integrated temperature sensors have been widely developed over the past decade, especially for thermal management. The sensors have been implemented with CMOS-compatible devices, such as BJTs, MOSFETs, resistors, and thermal diffusivity (TD). The conventional BJT-based temperature sensors are noted by their high accuracy [1], but cannot be scaled with modern CMOS processes. This is because they are based on the parasitic p-n-p or n-p-n transistors, which is very difficult to realize in the nanometer CMOS, and their base-emitter voltages are not scalable with low supply voltage. The MOSFETs, which are used with exponential behavior in the sub-threshold region [2, 3], can be a good alternative to operate at low supply voltage. However, the accuracy of such sensors is limited at high temperature due to leakage currents. The TD-based temperature sensors [4] are scalable with scaled CMOS process, operate well at low supply voltages, and can achieve moderate accuracy. However, they consume too much power, up to a few mW, making them difficult to use for such applications.

Recently, as shown in Fig. 1, temperature sensors based on on-chip resistors have proven to be extremely energy-efficient and have a high resolution comparable to other mature CMOS temperature sensors [16]. The resistor-based temperature sensors can be used for the on-chip thermal monitoring in microprocessors and DRAMs, which should be implemented with a moderate resolution, a very small area and high energy- efficiency (See Fig. 1 bottom-right). On the other hand, they can be used for the compensation in high-performance frequency reference, which should have an extremely high temperature resolution (sub-mK) [5, 6] (See Fig. 1 top-left).

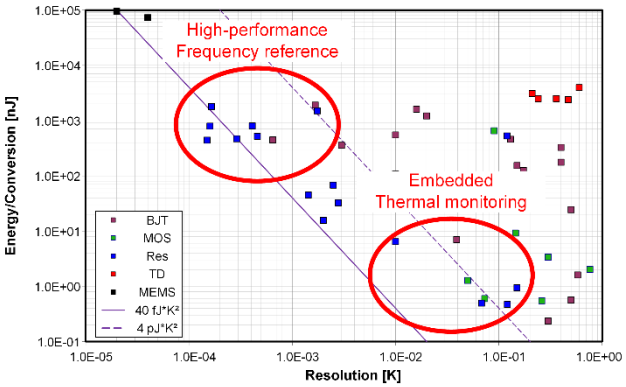

Fig. 1. Resistor-based temperature sensor performance comparison with CMOS temperature sensors

This paper provides a technical overview of various resistor-based temperature sensors. The temperature-dependent resistors can be built around several sensor compositions, such as Wheatstone bridges (WhB) [5]-[9], Wien-bridge (WB) [10, 11], RC networks [12, 13], and poly phase filters (PPF) [14, 15]. Each composition can be implemented with different readout interfaces, such as a continuous time ΔΣ ADC, a ratio-metric ADC, a phase-domain ΔΣ ADC, a single-slope ADC, and a frequency-locked loop. Each sensor has different pros and cons, so it is important to choose which methods to use for proper application. The rest of the paper is organized as follows. Section II explains characteristics of resistors in the CMOS process. Section III describes various resistor-based temperature sensors. Finally, the conclusion is presented in Section IV.

II. RESISTORS AS TEMPERATURE SENSING ELEMENTS IN CMOS

A. Resistor properties in CMOS process

There are many different options for resistors in CMOS processes: metal, diffusion, N-well, and polysilicon (poly) resistors. For temperature sensors, the sensing resistor should have a large temperature coefficient (TC) for high sensitivity, a large sheet resistance for smaller area, and low supply dependency and stress sensitivity for stable

a. Corresponding author: ychae@yonsei.ac.kr

Manuscript Received Nov. 13, 2020, Revised Dec. 28, 2020, Accepted Dec. 29, 2020

operation. The properties of resistors are summarized in Table I.

The metal resistors have quite large TCs up to 0.4%/°C, but the sheet resistance of such resistors is very low. This leads to a large chip area or a large power consumption. The resistance of diffusion resistors highly depends heavily on their doping level and the reverse-bias voltage between themselves and the well diffusion. The N-well resistors have comparable TCs to metal resistors and very low 1/*f* noise, but have very low doping levels, which can be an issue in stability.

The poly-silicon resistors have small TCs and exhibit large 1/f noise. However, the silicide layer can be added to poly and diffusion resistors. The silicide is a highly conductive silicon-metal alloy, resulting in its property of between metal and silicon resistors. Compared to non-silicide resistors, silicided poly (S-poly) one have relatively large TCs comparable to metal resistors, low 1/*f* noise, low supply dependency, and low stress sensitivity. However, they have a very low sheet resistance leading to a large chip area.

The S-poly resistors are often used as temperature sensing elements due to their high TC and stability over a wide temperature range. As shown in Table II, the properties of the S-poly resistors in two different process nodes (0.18-µm and 65-nm CMOS) are compared. In both process nodes, the implementation of the silicide increases their TCs (0.28~0.3%/°C), comparable to metal resistors. However, the sheet resistance in the 65-nm CMOS is 2× larger than that in the 0.18-µm node, resulting in a proportionally smaller size. Despite the larger non-linearity in 65-nm CMOS, this can be corrected in the digital backend of the sensor interface. In conclusion, it can be said that the S-poly resistors are the best choice for the temperature sensing elements.

TABLE I. Properties of resistors in CMOS process.

Resistor Type	Metal	Diff.	N-well	Poly	S-poly
TC	Large	Medium	Large	Medium	Large
Sheet R	Very small	Large	Large	Large	Medium
Supply dependency	Small	Medium	Large	Small	Small
1/*f* noise	No	No	No	Large	Small
Stress sensitivity	Small	Large	Large	Medium	Small

TABLE II. Properties of S-poly resistors in different CMOS processes.

Process Type	0.18-µm	65-nm
TC	Large (~ 0.3 %/°C)	Large (~ 0.28 %/°C)
Sheet R	Highly small (< 0.1 Ω/□)	Small (< 0.2 Ω/□)
Non-linearity	Small	Large

B. Systematic nonlinearity and process corner variations

The systematic nonlinearity of the resistor can be critical in temperature inaccuracy across process variations. Fig. 2 shows the procedure of systematic nonlinearity correction. It is simulated with silicided p-poly resistors in TSMC 65nm-CMOS. The simulated resistances with 13 temperature points in each corner are fit to the temperature by the 1st-order linear fit based on the mean value of 50 samples. After the linear fit, the rest of nonlinearity, shown in Fig. 2 (b), which is mainly due to the nonlinearity of resistor's TC, can be considered as a systematic error. This can be removed by a fixed polynomial fit. Fig. 2 (c) shows the residual temperature errors after systematic nonlinearity correction over process corners. As can be seen, the accuracy of temperature sensors can be improved by using a fixed polynomial correction.

Table III shows the comparison of a one-point trimmed temperature error with different polynomial in different process corners [15]. The best polynomial fit is based on each corner's own master curve, and the fixed polynomial fit is based on the simulated data in a typical corner. It should be noted that the 3σ error difference in each corner (FF, SS) is only ±0.07 °C and ±0.18 °C, respectively. It demonstrates that the systematic nonlinearity in each corner agrees well with a fixed polynomial fit that is based on the result of typical corner.

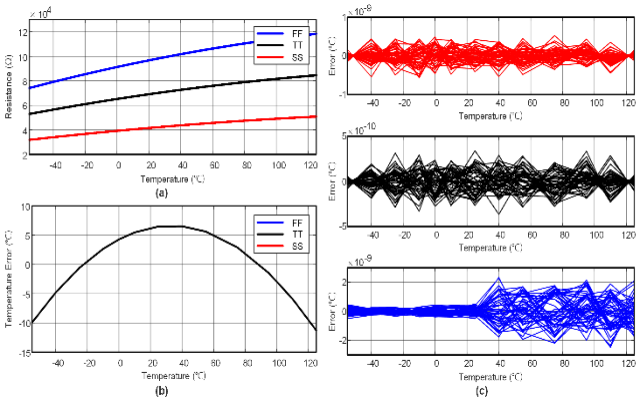

Fig. 2. The procedure of systematic nonlinearity correction for resistor-based sensors (a) corner variations (b) systematic non-linearity (c) residual temperature errors after systematic non-linearity correction.

TABLE III. One-point trimmed 3σ inaccuracy comparison (from [15])

Process Corner	1-point trimmed 3σ inaccuracy		Difference (3σ)
	w/ fixed polynomial fit	w/ best polynomial fit	
FF	±1.63 °C	±1.56 °C	±0.07 °C
SS	±1.96 °C	±1.78 °C	±0.18 °C

III. RESISTOR CONFIGURATION & READOUT INTERFACE IN RESISTOR-BASED TEMPERATURE SENSORS

It is important to find the best combination of resistor configuration and the following readout interfaces. This section describes four representative combinations: Wheatstone bridge (WhB) sensors, Wien-bridge (WB) sensors, RC network-based sensors, and polyphase filter (PPF) sensors.

A. Wheatstone bridge & ADC readout

As shown in Fig. 3(a), a WhB sensor consists of two different resistors (R_1 and R_2) with positive and negative TCs to achieve high temperature sensitivity and thus high energy-efficiency. Two resistors are implemented as silicided p-poly and non-silicided n-poly resistors with opposite TCs [5]-[9]. The resistor R_3 connected to V_{DD} or ground cancels the WhB current (I_{WhB}). This can be used as a resistive DAC in the continuous time ΔΣ modulator. As shown in Fig. 3(b), the error signal (I_{err}) between I_{WhB} and I_{DAC} is integrated via an active integrator, and the quantizer triggers its output and switches the DAC's input current in a ΔΣ manner. The output current of the bridge can be compensated more precisely with multi-bit modulators [5, 6, 9]. If the quantization noise of the modulator is effectively removed, the output noise will only be affected by the thermal noise of the WhB sensor, ensuring both high resolution and high energy-efficiency. However, the use of the active integrator often requires the large-area integration capacitor and the power-hungry opamps. Therefore, this sensor can achieve a high resolution, but with large area consumption.

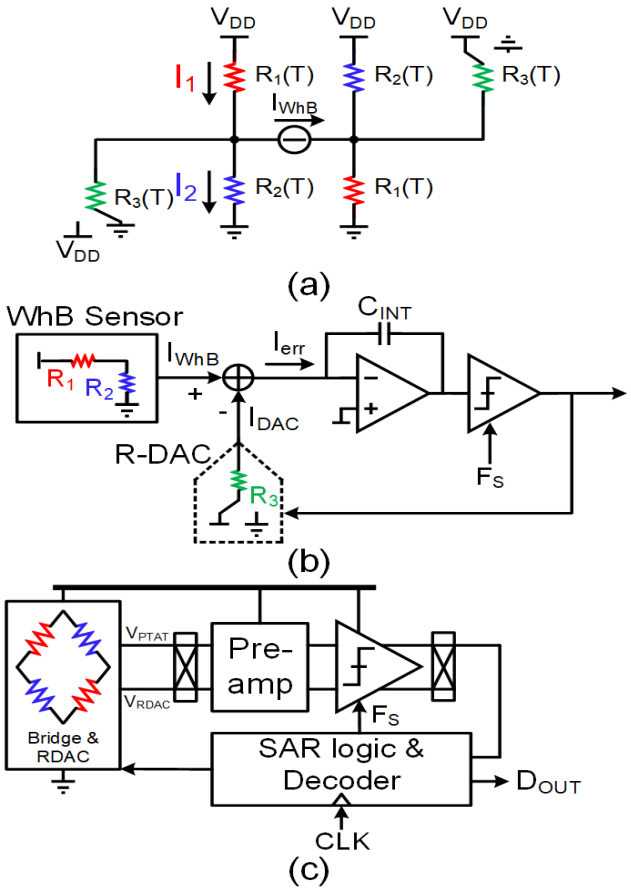

Fig. 3. WhB-based sensor: (a) WhB configuration, (b) Continuous time ΔΣ ADC readout and (c) SAR-assisted ratio-metric ADC readout.

On the other hand, as shown in Fig. 3(c), the ratio-metric measurement technique can be used with a SAR-assisted readout [7]. This improves the supply sensitivity. In this structure, re-using the WhB sensor as a reference DAC inherently removes the supply dependency of the sensor. The output voltages from the WhB sensor feed to the comparator with pre-amplifier, which consists of a 10-bit SAR ADC. In this architecture, a low supply sensitivity (0.28°C/V) and low power consumption (47μW) was achieved from 0.8-V supply voltage. However, the temperature resolution is limited by quantization noise leading to relatively low resolution (121 mK) with a large area consumption (0.044 mm^2).

B. Wien-bridge & CCO-based Phase-domain ΔΣ ADC

Fig. 4 shows the schematic of the Wien-bridge (WB) sensors and CCO-based phase-domain ΔΣ ADC [10, 11]. In a single-ended configuration, it consists of two S-poly resistors (R_1) and two capacitors. The bridge works as a passive 2^{nd}-order bandpass filter. When driven at a fixed frequency $F_{WB}= f_0$, the WB's output current I_{WB} has the phase shift information, which can be converted into the temperature information.
In the phase-domain ΔΣ modulator, the reference voltage is replaced by a reference phase with the same frequency with F_{WB}. Unlike a conventional analog phase-domain ΔΣ modulator, the CCO-based phase-domain ΔΣ modulator was proposed to digitize the WB current [11] with much smaller area consumption. The WB is modulated by the F_{WB}, and its output drives a current-controlled oscillator (CCO). The CCO only converts the I_{WB} to the frequency domain. It should be noted that the loop filter of this modulator is implemented as a digital up/down counter. When the counter is clocked by the CCO output, the phase DAC output ϕ_{DAC} is integrated with the up/down counter. Then, since the MSB of the counter (D_{OUT}) determines the polarity of the integration, it works as a quantizer of the modulator. Finally, the average of the ϕ_{DAC} values controlled by D_{OUT} balances out the input phase shift of the WB. In this structure, the all-digital readout removes the active circuits, thus resulting in a very small area (0.0068 mm^2). However, due to the time-discretization noise of the counter, its resolution is limited by the clock frequency of the counter, which shows a direct tradeoff between the resolution and the power consumption

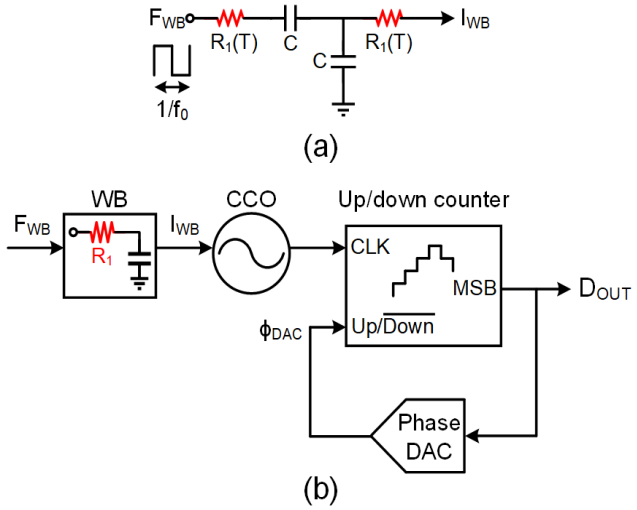

Fig. 4. WB-based sensor: (a) WB configuration and (b) CCO-based phase-domain ΔΣ ADC readout.

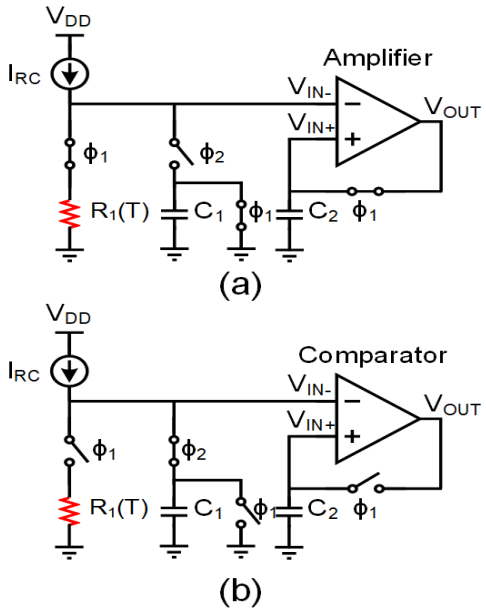

Fig. 5. RC-based sensor operation: (a) Sensing phase and (b) Conversion phase.

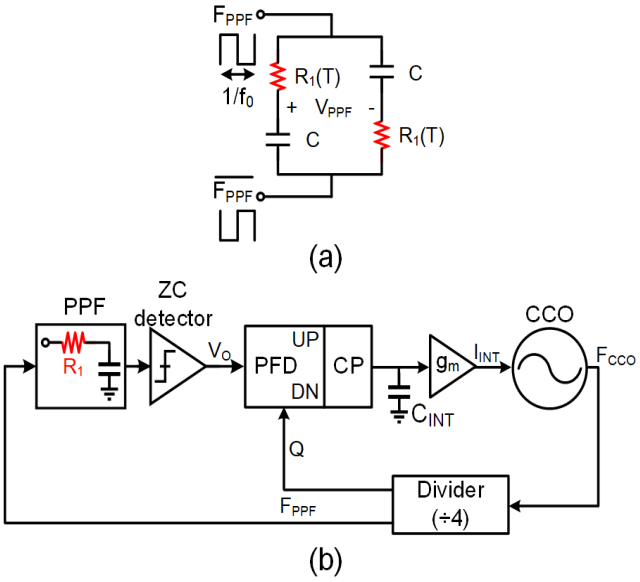

Fig. 6. PPF-based sensor (a) PPF configuration and (b) Frequency locked-loop readout.

C. RC network & Single-Slope ADC

Fig. 5 shows the operation of the RC-based sensor [12]. The network consists of a sensing resistor R_1, a capacitor C_1, and the bias current I_{RC}. As shown in Fig. 5(a), the sensor's operation is divided into two phases: sensing (ϕ_1) and conversion (ϕ_2). During the sensing phase, the R_1 is connected to the I_{RC}, the C_1 to ground for the reset, and the amplifier is configured as a unit-gain buffer. Thus, the C_2 samples a temperature-dependent signal voltage from R_1 and I_{RC}. During the conversion phase, the I_{RC} is connected to the C_1 and charges. The amplifier output can be converted as a comparator. When the V_{IN-} reaches the voltage saved in previous phase, the comparator toggles its output and generates a temperature-dependent periodic signal which is digitized by an output counter as a single-slope ADC. By reusing the amplifier and a bias circuit, the sensor's area ($0.01mm^2$) and power ($12.8\mu W$) can be minimized. If a high-speed clock for the counter (e.g. 100MHz in [12]) is available in the system, a small RC value can then be used, which ensures the short conversion time and low energy consumption. However, the sensor's resolution (150mK) is often limited by the quantization noise of the ADC.

D. Polyphase Filter & Frequency-locked-loop

As shown in Fig. 6(a), the polyphase filter (PPF) sensor consists of a pair of S-poly resistors and capacitors [14, 15]. The two ends of PPFs are driven by an anti-phase clocks F_{PPF}. The PPF output voltage V_{PPF} has the temperature-dependent phase shift. Compared to a differential WB sensor, this PPF sensor has a larger output swing and a larger phase shift. This enables a very small area implementation [14, 15]. In order to effectively utilize the properties of the PPF, the zero-crossing (ZC) detector and the frequency-locked-loop (FLL) readout are used. The ZC point of the differential output of the PPF is detected by the ZC detector. The output frequency of the CCO is divided by 4 to provide an in-phase signal for driving PPF (F_{PPF}) and a quadrature-phase signal (Q) for the phase-frequency detector (PFD). The PFD outputs a phase error between the ZC detector output and the Q-signal. The digital tri-state PFD generates up/down signal to provide it into the charge pump (CP), whose current output is fed into the integration capacitor (C_{INT}). The voltage on the C_{INT} is converted into the driving current of the CCO. At steady state, the current is adjusted to make the phase error become zero and the output frequency F_{CCO} is locked to four times the PPF center frequency.

In this structure, the use of the ZC detector and the PFD further reduces the sensor's area (0.007 mm^2 [14] and 0.0058 mm^2 [15]) in the advanced process nodes. Also, thanks to the noise reduction of the sensing front-end in the FLL, the resolution (2.5 mK [14] and 2.8 mK [15]) of the sensor can be improved. However, the flicker noise of the ZC detector and the charge pump is dominant noise source of the sensor. To improve the noise performance of this sensor without increasing their size, an additional chopping technique can be used as in [13].

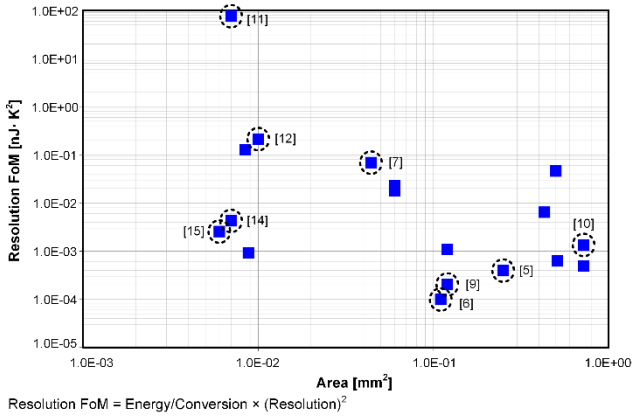

Fig. 7. Performance comparison with resistor-based temperature sensors (Resolution FoM versus area)

E. Performance comparison

Fig. 7 shows the performance comparison for resistor-based temperature sensors, which is based on the resolution FoM versus the silicon area. The resolution FoM is defined as Energy/Conversion × (Resolution) ^{2}, which represents the energy-efficiency of the temperature sensors [16]. The WhB-based sensor with a CT ΔΣ ADC achieved the best FoM of 10 fJ·K^2, but with a large area of 0.11 mm^2 [6]. The WhB-based sensor with a ratio-metric ADC was implemented in a much smaller area of 0.044 mm^2, but suffered from the degradation in the energy efficiency (FoM =6.9 pJ·K^2) [7]. The WB-based sensor with CCO-based phase-domain ΔΣ ADC was implemented in a much smaller area (0.0068 mm^2), but was not energy-efficient (FoM =7.6 nJ·K^2) [11]. The RC-based sensor with a single-slope ADC was also implemented in a small area of 0.01 mm^2, but the energy-efficiency was not good (FoM = 20 pJ·K^2) [12]. Finally, the PPF-based sensor with a FLL readout achieved a good FoM of 260 fJ·K^2 and a small area of 0.0058 mm^2 [15].

IV. CONCLUSION

This paper provides an overview of recent advances in resistor-based temperature sensors. The silicided poly resistors have proven to be the most suitable for the sensing elements because of their relatively high TCs, low 1/f noise, low supply dependency, and low stress sensitivity. A performance comparison of the resistor-based temperature sensors is also given for various sensor configuration and readout interfaces based on the resolution FoM and the silicon area. It turns out that the resistor-based temperature sensors can be implemented in an area- and energy-efficient manner and can then be used for many applications.

REFERENCES

[1] K. Souri, Y. Chae, and K.A.A. Makinwa,"A CMOS Temperature Sensor with a Voltage-Calibrated Inaccuracy of ±0.15°C (3σ) from -55°C to 125°C," *IEEE J. Solid-State Circuits*, vol. 48, no. 1, pp. 292–310, Jan. 2013.

[2] Y. Kim et al., "A 0.02mm^2 embedded temperature sensor with ±2°C inaccuracy for self-refresh control in 25nm mobile DRAM," in Proc. *ESSCIRC*, Sep. 2015, pp. 267–270.

[3] S. Park et al., "A DTMOST-based Temperature Sensor With 3σ Inaccuracy of ±0.9°C for Self-Refresh Control in 28nm Mobile DRAM," in *IEEE Custom Integrated Circuits Conference (CICC)*, Mar. 2020.

[4] U. Sönmez, F. Sebastiano, and K. A. A. Makinwa, "Compact Thermal-Diffusivity-Based Temperature Sensors in 40-nm CMOS for SoC Thermal Monitoring," *IEEE J. Solid-State Circuits*, vol. 52, no. 3, pp. 834-843, Mar. 2017.

[5] S. Pan and K. A. A. Makinwa, "A 0.25mm^2 Resistor-Based Temperature Sensor with an Inaccuracy of 0.12°C (3σ) from -55°C to 125°C and a Resolution FOM of 32fJ·K^2," *IEEE J. Solid-State Circuits*, vol. 53, no. 12, pp. 3347-3355, Oct. 2018.

[6] S. Pan and K. A. A. Makinwa, "A 10 fJ·K^2 Wheatstone Bridge Temperature Sensor With a Tail-Resistor-Linearized OTA," *IEEE J. Solid-State Circuits*, Early Access, Sep. 2020.

[7] H. Park and Jintae Kim, "A 0.8-V Resistor-Based Temperature Sensor in 65-nm CMOS With Supply Sensitivity of 0.28 °C/V," *IEEE J. Solid-State Circuits*, vol. 53, no. 3, pp. 906-912, Mar. 2018.

[8] H. Xin, M. Andraud, P. Baltus, E. Cantatore, and P. Harpe, "A 174 pW–488.3 nW 1 S/s–100 kS/s All-Dynamic Resistive Temperature Sensor With Speed/Resolution/Resistance Adaptability," *IEEE Solid-State Circuits Lett.*, vol. 1, no. 3, pp. 70–73, Apr. 2018.

[9] S. Pan and K. A. A. Makinwa, "A Wheatstone Bridge Temperature Sensor with a Resolution FoM of 20fJ·K^2," in *IEEE Int. Solid-State Circuits Conf. (ISSCC) Dig. Tech. Papers*, Feb. 2019, pp. 186–188.

[10] S. Pan and K. A. A. Makinwa, "A Resistor-Based Temperature Sensor With a 0.13 pJ·K^2 Resolution FoM," *IEEE J. Solid-State Circuits*, vol. 53, no. 1, pp. 164-173, Sep. 2017.

[11] J. Angevare and K. A. A. Makinwa, "A 6800-μm^2 resistor-based temperature sensor in 180-nm CMOS," *IEEE J. Solid-State Circuits*, vol. 54, no. 10, pp. 2649-2657, July. 2019.

[12] A. Mordakhay and J. Shor, "Miniaturized, 0.01 mm^2, Resistor-based Thermal Sensor with an Energy Consumption of 0.9 nJ and a Conversion Time of 80 μs for Processor Applications," *IEEE J. Solid-State Circuits*, vol. 53, no. 10, pp. 2958-2969, Aug. 2018.

[13] A. Khashaba, J. Zhu, A. Elmallah, M. Ahmed, and P. K. Hanumolu, "A 0.0088mm^2 Resistor-Based Temperature Sensor Achieving 92fJ·K^2 FoM in 65nm CMOS," in *IEEE Int. Solid-State Circuits Conf. (ISSCC) Dig. Tech. Papers*, Feb. 2020, pp. 60–61.

[14] W. Choi, et al., "A Compact Resistor-Based CMOS Temperature Sensor With an Inaccuracy of 0.12 °C (3σ) and a Resolution FoM of 0.43 pJ·K^2 in 65-nm CMOS," *IEEE J. Solid-State Circuits*, vol. 53, no. 12, pp. 3356-3367, Dec. 2018.

[15] Y. Lee, et al., "A 5800μm^2 resistor-based temperature sensor with a one-point trimmed inaccuracy of ±1.2 °C (3σ) From −50 °C to 105 °C in 65-nm CMOS," *IEEE Solid-State Circuits Lett.*, vol. 2, no. 9, pp. 67–70, Sep. 2019.

[16] K. A. A. Makinwa. Smart Temperature Sensor Survey. Accessed: Nov. 4, 2020. [Online]. Available: http://ei.ewi.tudelft.nl/docs/TSensorsurvey.xls

Yong Tae Lee received the B.S. degree in electrical and electronic engineering from Yonsei University, Seoul, South Korea, in 2016, where he is currently pursuing the Ph.D. degree in electrical and electronic engineering. His current research interests include low-power, high-accuracy temperature sensors.

Woo Jun Choi received the B.S. degree in electrical and electronic engineering from Yonsei University, Seoul, South Korea, in 2015, where he is currently pursuing the Ph.D. degree in electrical and electronic engineering. He is being supported by the National Research Foundation of Korea (NRF) Grant funded by the Korean Government (NRF-2016-Global Ph.D. Fellowship Program). His current research interests include high-speed interface circuits, precision analog circuits, and CMOS temperature sensors.

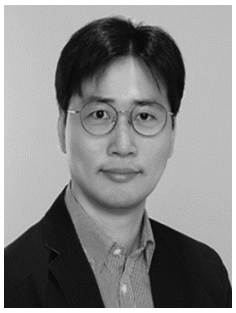

Young Cheol Chae received the B.S., M.S., and Ph.D. degrees in Electrical and Electronic Eng. from Yonsei University, Seoul, Korea, in 2003, 05, and 09, respectively. From 2009 to 2011, he was a Post-Doctoral Researcher in Delft University of Technology, Delft, The Netherlands.

Since 2012, he has been a faculty with Yonsei University and is currently an Associate Professor. He focused on low-power data converters and high-performance sensor interfaces. This results in more than 90 technical papers and 30 patents.

Dr. Chae is an active member of the Technical Program Committees of the International Solid-State Circuits Conference (ISSCC) and the Asian Solid-State Circuits Conference (A-SSCC). He is a Distinguished Lecturer (DL) of the IEEE Solid-State Circuits Society (SSCS) in 2018-2019. He received the Best Young Professor Award in engineering from Yonsei University in 2018, the Haedong Young Engineer Award from IEE Korea in 2017, the Outstanding Research Award of Yonsei University in 2017/18/19, the Outstanding Teaching Award of Yonsei University in 2013/14, a Research Grant from the Samsung Research Funding Center in 2017, and the VENI Grant from the Dutch Technology Foundation STW in 2011.